

Optical Control of Coherent Interactions between Electron Spins in InGaAs Quantum Dots

S. Spatzek,¹ A. Greulich,^{1,*} Sophia E. Economou,² S. Varwig,¹ A. Schwan,¹ D. R. Yakovlev,^{1,3} D. Reuter,⁴
A. D. Wieck,⁴ T. L. Reinecke,² and M. Bayer¹

¹*Experimentelle Physik 2, Technische Universität Dortmund, D-44221 Dortmund, Germany*

²*Naval Research Laboratory, Washington, D.C. 20375, USA*

³*A. F. Ioffe Physico-Technical Institute, RAS, St. Petersburg, 194021 Russia*

⁴*Angewandte Festkörperphysik, Ruhr-Universität Bochum, D-44780 Bochum, Germany*

(Received 9 November 2010; published 21 September 2011)

Coherent interactions between spins in quantum dots are a key requirement for quantum gates. We have performed pump-probe experiments in which pulsed lasers emitting at different photon energies manipulate two distinct subsets of electron spins within an inhomogeneous InGaAs quantum dot ensemble. The spin dynamics are monitored through their precession about an external magnetic field. These measurements demonstrate spin precession phase shifts and modulations of the magnitude of one subset of oriented spins after optical orientation of the second subset. The observations are consistent with results from a model using a Heisenberg-like interaction with μeV strength.

DOI: [10.1103/PhysRevLett.107.137402](https://doi.org/10.1103/PhysRevLett.107.137402)

PACS numbers: 78.67.Hc, 78.47.jh

Considerable progress has been made recently in establishing optical control of spins confined in semiconductor quantum dots (QDs), a system of interest for quantum bits (qubits) in implementations of quantum information [1]. Single spin decoherence times on the order of microseconds have been demonstrated [2], and methods for spin initialization and readout have been developed [3,4]. Recently, progress in demonstrating optical rotations of single spins has been made [5–8]. To be useful in quantum information, spin manipulation times must be orders of magnitude faster than decoherence times [1], which is possible by using fast optical methods. Interactions between spins in QD systems can provide the mechanism for coherent control in quantum logic but can also complicate their coherent dynamics. The case of coupling between spins in QD molecules has been well studied [9–12], but long-ranged interactions are not yet understood.

An ensemble of QDs has the advantage of having strong optical coupling, but ensemble approaches typically have been hampered by inhomogeneities in their properties, particularly spin splittings, which lead to fast spin dephasing. In previous work we have demonstrated nuclear-assisted optical techniques for removing some of the effects of these inhomogeneities [2,13]. In these techniques, periodic pulse trains orient spins normal to an external magnetic field, and particular subsets of spins precess in phase with the pulse trains. At rather low magnetic fields, around $B = 1$ T, a spin ensemble can be put into a state in which only few spin precession modes contribute [14]. This is the system that we study here.

In the present work, two subsets of spins are selected by spectrally narrow, circularly polarized laser pulse trains of different photon energies. The subsets are oriented by the two laser pulses (pump 1 and pump 2) and precess around a perpendicular magnetic field. The relative phase of the two

precessions is controlled by the time difference between the two pulses. We find that, after the second pump pulse, the precession associated with the first spin subset acquires a phase shift that depends on the relative orientation of the spins. It emerges smoothly in time after pump 2. In addition, the precession amplitude shows modulations and decreases with time. The major experimental features are consistent with a Heisenberg-like interaction between the spins in the ensembles with strength on the order of μeV .

The experiments were performed on an ensemble of self-assembled (In, Ga)As/GaAs QDs grown by molecular beam epitaxy such that each QD contains on average a single electron. The sample contained 20 layers of dots with 60 nm separation between adjacent layers and a sheet dot density of 10^{10} cm^{-2} [15]. The experiments were performed at $T = 6$ K in a magnetic field of 1 T. The spin dynamics were investigated by time-resolved ellipticity, which measures the spin projection along the optical axis (the z direction), which coincides with the QD growth direction. The sample was excited by two phase-synchronized trains of pump laser pulses with a time jitter well below 1 ps. The pump lasers were tuned to different energies in the inhomogeneously broadened QD photoluminescence, as sketched in Fig. 1(a). The laser pulses were emitted at a frequency of 75.75 MHz and had durations of 2 ps corresponding to 1 meV spectral width. The circular polarizations of the two lasers were adjusted independently, as was the delay between them. For ellipticity studies, a weak probe was split from one of the pumps, and after being polarized linearly it was sent through the sample. The change of probe polarization ellipticity was recorded by a balanced detection scheme [2].

The circularly polarized optical pulse of intensity π excites the QD spin to a trion state leaving the other spin to precess around a perpendicular magnetic field applied

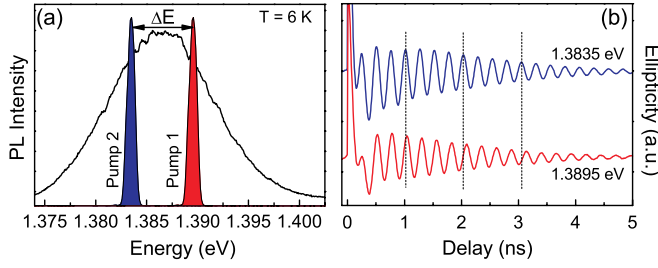


FIG. 1 (color online). (a) Photoluminescence spectrum of the (In,Ga)As QD sample. Two shaded areas give line shapes of the picosecond laser pulses at energies 1.3835 and 1.3895 eV used to initialize two subsets of spins. (b) Ellipticity traces of the two different spin subsets. At early delays < 500 ps, the signals show some weak exciton interference from neutral QDs.

along the x direction [15]. Figure 1(b) gives ellipticity results with a single pump laser exciting the QD ensemble that is probed at the same energy. In the upper trace the pump and probe photon energy were on the low energy side of the photoluminescence band, and in the lower trace they were shifted to the high energy side by $\Delta E \sim 6$ meV. In both cases, the pump laser creates spin coherence at time zero after which the electron spin precesses. We estimate that there are about 10^6 spins in each subset corresponding to an average separation exceeding 90 nm between the spins. Note that the precession frequencies are different from one another due to the difference in their electron g factors.

In the two-pump laser experiments, about the same spacing as in Fig. 1(a) was used for the two pump energies, so that the pulses had no spectral overlap. The lasers therefore orient the spins in distinct subsets of QDs. The pulses were sufficiently detuned so that no spin rotation of one spin subset by the laser exciting the other subset could be resolved [8,16,17]. The signature of such a rotation would be an instantaneous phase shift at the time of laser pulse.

Figure 2(a) gives results when two circularly polarized pulses are applied with a fixed time difference between them for each trace. The probe energy used to measure the spin coherence was the same as that of pump 1. Thus the effect of the spins driven by pump 2 on those driven by pump 1 is monitored. The black curve is a reference trace with only pump 1 on. The incidence times of pump 2 are given by the dots on the reference trace.

For the bottom pair of traces in Fig. 2(a), pump 2 is applied when the reference trace is at a minimum so that spin subset 1 is pointing in the $-z$ direction. Red (gray) and blue (dark gray) traces are for the two circular polarizations of pump 2 creating spins that point along the $+z$ or the $-z$ direction, respectively. Phase shifts with respect to the reference emerge after pump 2 and have opposite signs for the two polarizations of pump 2. The slow, nearly linear emergence of phase shifts with increasing probe delay time after pump 2 is shown in Fig. 2(b). This slow time

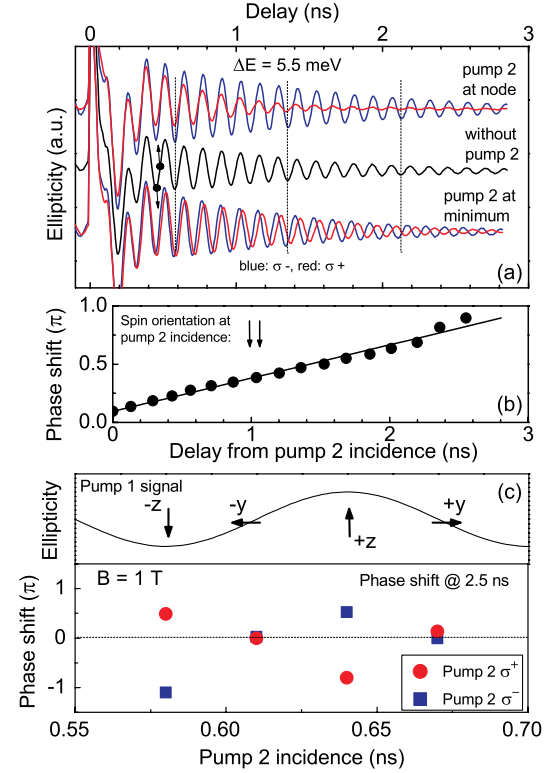


FIG. 2 (color online). (a) Ellipticity as function of time delay for two pumps. (b) Phase shift evolution in time after pump 2 for collinear spin orientations. (c) Phase shift as a function of incidence times of pump 2. The black curve is a reference trace, and arrows indicate orientations of spin subset 1 when pump 2 is applied. Phase shifts are measured at 2.5 ns probe delay.

dependence excludes its resulting from rotation of subset 1 by laser 2. The top pair of traces corresponds to pump 2 being applied when the ellipticity signal is zero, i.e., when spin subset 1 points along the $-y$ direction. In this case the phase shifts are small.

The dependences of the phase shifts on the polarizations of pumps 1 and 2 are given in Fig. 2(c). Pump 1 had σ^+ polarization, and pump 2 had σ^+ or σ^- polarizations. The incidence time of pump 2 was varied to provide different orientations of spin subset 1, which are indicated by the black arrows on the top. The phase shifts are essentially zero when spin subsets 1 and 2 are perpendicular at pump 2. They are large when subset 1 is along $+z$ or $-z$, and they are of opposite sign for σ^+ and σ^- polarizations of pump 2.

Additional interesting features appear when the signal is monitored over longer delays up to 4 ns for the cases of large phase shifts. These results are shown in Fig. 3(a). The black (top) and green (3rd from the top) traces in the left panel give the ellipticity after excitation by a single pump laser so that only spin subset 1 or subset 2 is oriented. The delay of 390 ps between the two pumps is the same as in the two-pump experiments described below. In the single-pump experiments, we observe a decay of the envelope of the z spin component with increasing delay. We associate

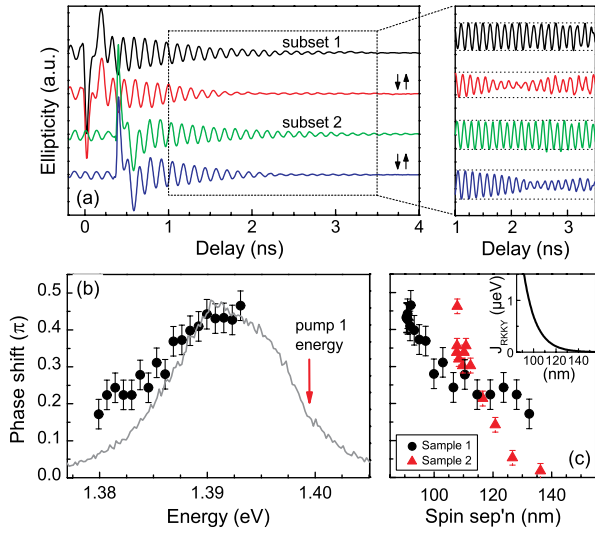


FIG. 3 (color online). (a) The left panel gives ellipticity for single pump-probe measurements of spin subset 1 at 1.39 eV (black) and spin subset 2 at 1.385 eV (green, 3rd from top). The red (2nd) and blue (4th) curves are for two pumps with probe at the energy of pump 1 or 2, respectively. The right panel gives a zoom-in of time dependences with the exponential decay component removed (see the text). (b) Phase shift as a function of detuning between pumps at one sample position. (c) Phase shift as a function of spin separation for two measured samples. (Inset) Interaction strength J_{RKKY} as a function of spin separation.

this decay with dephasing due to inhomogeneous spin precession. This dephasing is weak because at 1 T magnetic field each spin subset precesses with a number of modes close to 1 [13]. The ellipticity envelope after trion decay can be fitted accurately by an exponential with a dephasing time $T_2^* = 0.8$ ns.

The red (2nd from top) and blue (4th) traces in Fig. 3(a) give the ellipticities when both pump 1 and pump 2 are applied, with the probe on spin subset 1 for the red (2nd) trace and on spin subset 2 for the blue (4th) trace. The initial directions of spin subsets 1 and 2 are given by the arrows. In each case we see small but clear modulations of the signal near 2.5–3 ns. These features are clearer when we remove the exponential decay due to dephasing [15] using the time T_2^* from the single-pump measurements. The results are shown in the right portion of Fig. 3(a). For the black and green (3rd) curves with only one pump, we see harmonic oscillations without modulation. There are two distinct features from the red (2nd) and blue (4th) traces with two pumps: a modulation of the magnitudes of the envelopes and a decay of the envelope of ellipticity compared to the one-pump cases.

The power dependence of the phase shifts is shown in Fig. 4(d), where the phase shift increases with power up to pulse area of π and decreases thereafter.

In order to understand these results, we consider a spin system with optical pulses and with interactions between the spins. For simplicity, we consider a model of two spins

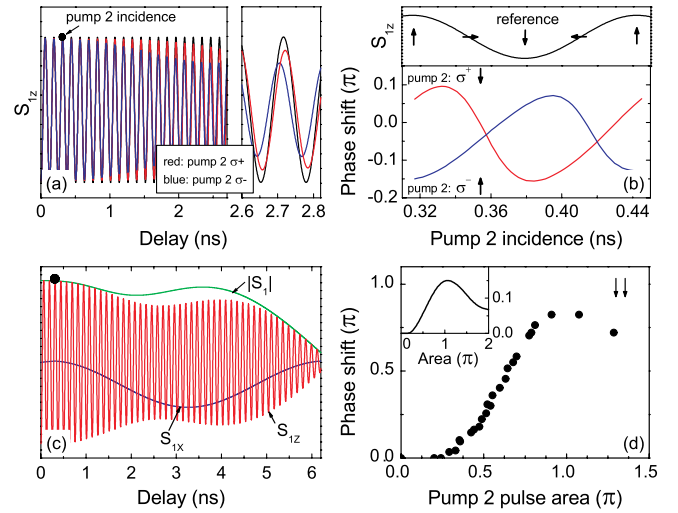


FIG. 4 (color online). Calculations for (a) spin polarization along the optical axis z as a function of delay time from pump 1. The right panel shows (zoom-in) extended time period and phase shifts. (b) Phase shifts at a probe delay time of 2.5 ns for σ^+ and σ^- polarizations of pump 2; incidence times such that spin 1 is oriented as shown by arrows in the top panel. (c) Expectation values of S_{1z} , S_{1x} , and $|S_1|$. (d) Measured phase shift as a function of pump 2 power. (Inset) Calculated power dependence of the phase shifts.

interacting with a Heisenberg form $J\mathbf{S}_1 \cdot \mathbf{S}_2$ where the spins are subject to separate periodic optical pulse trains of different energies. Here J is the interaction strength, and \mathbf{S}_1 and \mathbf{S}_2 are the spin operators.

We solve for the steady state dynamics of the system, which is done by constructing the evolution operator for the combined system, obtaining the corresponding density matrix, and propagating it forward in time to the joint steady state. The expectation value of spin 1 as a function of time is obtained by tracing out spin 2 from the density matrix. Dephasing from the environment is not included here, and as a result there is no loss of amplitude in time from sources outside of the spin system. We have considered the effects of other unpolarized spins by using a simple model and find that they do not affect the qualitative features of the response [18].

Results from these calculations are given in Fig. 4. Figure 4(a) gives the time dependence of expectation value S_{1z} . The black reference trace is for only pump 1 applied. The dot indicates the time of pump 2, when the reference spin is in the $+z$ direction. Red (gray) and blue (dark gray) traces are for σ^+ and σ^- polarizations for pump 2. The extended panel in Fig. 4(a) shows the two phase shifts emerging smoothly and approximately linearly in time after pump 2. Figure 4(b) gives the phase shifts for varying times of application of pump 2 for the two pump 2 polarizations. We see that the phase shifts for the two polarizations of pump 2 are opposite in sign. These phase shifts are absent without the interaction J . Asymmetries in the features arise from the two g factors being unequal.

Calculated results for a wider range of delay times are shown in Fig. 4(c). The curves give S_{1z} , S_{1x} , and $|S_1|$ of spin 1 after spin 2 is traced out of the density matrix. S_{1z} oscillates around the magnetic field with the Larmor frequency. In the absence of interactions between the spins, the envelopes of S_{1z} and $|S_1|$ would be constant in time, and S_{1x} would be zero. With interactions, the envelope of S_{1z} decreases in time and becomes modulated. In addition, the overall magnitude $|S_1|$ decreases in time. These features result from coupled dynamics of the two spins in the presence of the interaction. The inset in Fig. 4(d) shows the calculated phase shift as a function of pump 2 power. This behavior results from an oscillation of the spin polarization of subset 2 excited by pump 2, which subsequently interacts with spin subset 1.

We find that a value of $J \sim 1 \mu\text{eV}$ gives features qualitatively similar to those in the experiment in Fig. 2. We have also tried other forms of interactions between spins, including an Ising form. These forms give a number of results similar to those from the Heisenberg interaction but are in less good overall accord with the experiment.

We see that the key features from the experiment are consistent with the results of this model of interacting spins. The ellipticity in the experiments corresponds to the spin magnitude in the model. (i) In both cases the phase shifts emerge smoothly in time after the second optical pulse. In the model this behavior arises from the coupled dynamics of the two interacting spins, and it would not be present without the interaction. (ii) The dependence of the phase shifts on the polarizations of the two lasers is similar. In both cases for a fixed polarization of pump 1, the phase shifts are opposite in sign for σ^+ and σ^- polarizations of pump 2. In both cases the phase shifts are large when the spins are either parallel or antiparallel and small when they are perpendicular at the second pulse. (iii) The dependence of the phase shifts on the power of pump 2 in Fig. 4(d) is similar in the experiment and the model. In both cases the phase shift increases from low power, reaches a maximum near a pulse of π , and decreases after that. The fact that the phase shift of subset 1 follows the degree of spin polarization of subset 2 is associated with spin interactions. (iv) The modulations in magnitude of the ellipticity in the experiment correspond to the modulations of the spin magnitude in the model. These features result from the coupled dynamics of the spins in the presence of interactions.

From this list of similar features in the experiment and theory, we conclude that the experimental results give convincing evidence for the existence of interactions between the spins in these QD arrays.

The presence of interactions between spins is given added support from results for the dependence of the phase shifts on the separation between dots. The phase shifts measured at a fixed position on the sample as functions of the detuning between the two pumps are shown in Fig. 3(b) with the corresponding photoluminescence spectrum. The

arrow gives the position of pump 1, and the black dots the positions of pump 2. The photoluminescence intensities at pump 2 provide a measure of the number of dots excited at several energies.

The average separation between the spins is estimated from the number of excited dots. To do so, we include explicitly the separations of a given spin to spins within the layer and to those in two adjacent layers [18]. We find that including more distant spins does not affect the results significantly. The fraction of the dots that overlap the laser spectrally is determined by integrating the relevant regions of the photoluminescence spectrum. We determine the ratio of uncharged dots to the singly charged dots for each transition energy from the magnitudes of the Faraday rotations before and immediately after pump pulse application. The optically oriented electron spin density is obtained from the optically excited dot density at each energy by using this ratio. Finally, the average separation between spins is obtained from statistical averaging assuming that the dot distribution in a layer is Poissonian [18].

The phase shifts as functions of the average spin separation are shown by the black symbols in Fig. 3(c). The phase shifts decrease for increasing spin separation, as expected for a long-ranged interaction between spins. To support these results, an additional sample was studied (sample 2), which has a dot density 4 times higher than the first sample and a smaller interlayer separation of 30 nm. Results from this sample are shown by the red triangles in Fig. 3(c). The somewhat larger spin separation in that sample results from its larger spectral width and higher probability of doubly charged dots in it.

The present understanding of spin dynamics of these inhomogeneous arrays does not permit a definitive determination of the microscopic interaction mechanism between spins. Nevertheless, among all of the long-ranged spin interactions available, the optical RKKY interaction discussed in Refs. [19,20] is the only one that has an overall magnitude consistent with the value of interaction $J \sim 1 \mu\text{eV}$ obtained from the experiment [21]. To explore this further, we plot in the inset in Fig. 3(c) the dependence of the optical RKKY interaction, J_{RKKY} , between spins calculated as described in Ref. [20]. The resulting dependence of J_{RKKY} on spin separation is similar to the dependence of the observed phase shift on average spin separation. In addition, we note that the magnitude of J_{RKKY} is in the right μeV range for the parameters used [22].

In summary, we have presented evidence for coherent interactions between spins from pump-probe experiments on ensembles of InGaAs QDs and from calculations. These interactions can play important roles in coupling spins in quantum gates and in extended architectures for quantum information.

This work was supported by the BMBF project QuaHL-Rep, the Deutsche Forschungsgemeinschaft, the U.S. Office of Naval Research, and NSA/LPS. We acknowledge

helpful conversations with G. Ramon regarding the RKKY interaction.

*alex.greilich@udo.edu

- [1] G. Burkard, H. A. Engel, and D. Loss, *Fortschr. Phys.* **48**, 965 (2000).
- [2] A. Greilich *et al.*, *Science* **313**, 341 (2006).
- [3] M. Atatüre *et al.*, *Science* **312**, 551 (2006).
- [4] X. Xu *et al.*, *Phys. Rev. Lett.* **99**, 097401 (2007).
- [5] Y. Wu *et al.*, *Phys. Rev. Lett.* **99**, 097402 (2007).
- [6] J. Berezovsky *et al.*, *Science* **320**, 349 (2008).
- [7] D. Press, T. Ladd, B. Zhang, and Y. Yamamoto, *Nature (London)* **456**, 218 (2008).
- [8] A. Greilich *et al.*, *Nature Phys.* **5**, 262 (2009).
- [9] E. A. Stinaff *et al.*, *Science* **311**, 636 (2006).
- [10] H. J. Krenner *et al.*, *Phys. Rev. Lett.* **94**, 057402 (2005).
- [11] G. Ortner *et al.*, *Phys. Rev. Lett.* **94**, 157401 (2005).
- [12] D. Kim *et al.*, *Nature Phys.* **7**, 223 (2011).
- [13] A. Greilich *et al.*, *Science* **317**, 1896 (2007).
- [14] A. Greilich *et al.*, *Phys. Rev. B* **79**, 201305 (2009).
- [15] A. Greilich *et al.*, *Phys. Rev. Lett.* **96**, 227401 (2006).
- [16] S. E. Economou, L. J. Sham, Y. Wu, and D. G. Steel, *Phys. Rev. B* **74**, 205415 (2006).
- [17] S. E. Economou and T. L. Reinecke, *Phys. Rev. Lett.* **99**, 217401 (2007).
- [18] See Supplemental Material at <http://link.aps.org/supplemental/10.1103/PhysRevLett.107.137402> for the estimation of the average spin separation and the effects of coupling to multiple spins.
- [19] C. Piermarocchi, P. Chen, L. J. Sham, and D. G. Steel, *Phys. Rev. Lett.* **89**, 167402 (2002).
- [20] G. Ramon, Y. Lyanda-Geller, T. L. Reinecke, and L. J. Sham, *Phys. Rev. B* **71**, 121305(R) (2005).
- [21] We estimate that the classical dipolar interaction between spins for QD ensembles with average spin densities of $\sim 10^{10}/\text{cm}^2$ is much smaller, on the order of $10^{-9} \mu\text{eV}$, and interactions mediated by the nuclei should have an upper bound of $\sim 10^{-5} \mu\text{eV}$ due to slow nuclear spin diffusion between the dots.
- [22] The calculations were made by using a dot radius of 10 nm, a lateral confining potential of 150 meV, a detuning of 0.5 meV, and an optical coupling of 0.5 meV.